

Practical Aspects of On-Orbit Modal Identification Using Free-Decay Data

Axel Schenk*

German Aerospace Research Establishment (DLR), D-3400 Göttingen, Germany
and

Richard S. Pappa†

NASA Langley Research Center, Hampton, Virginia 23665

This paper discusses practical aspects of performing on-orbit modal identification using time domain analysis of free-decay data. The effects of environmental constraints, structural characteristics, excitation, and sensing are reviewed. In a recent laboratory application, an on-orbit experiment is simulated using a limited number of excitation and measurement points. The identified modal parameters correlate well, though not uniquely, with those obtained in a complete modal survey. Practical difficulties in performing the correlation are illustrated.

Introduction

MANY future space missions require large structures. Contrary to current spacecraft, these future structures will serve as platforms for simultaneous fulfillment of different tasks. An example is Space Station Freedom, shown in Fig. 1. Various payloads as well as structural variation during assembly will change vibrational properties. Furthermore, such systems are expected to operate over 20 years, during which time the configuration may change. For pointing precision, flight-path control, and vibration reduction, modal parameters of each assembly state are required.

Ground modal-survey tests are performed on all aerospace vehicles for updating analytical predictions. However, future large spacecraft such as the space station cannot be tested as a total structure on Earth. Size, zero-g design, and the existing atmosphere conflict with traditional structural dynamic testing. On-orbit modal identification will become necessary.¹

Traditional ground test methods will be difficult or impossible to apply in space. The classical phase resonance method is generally unsuitable because different shaker locations are necessary for exciting different modes, resulting in a large number of total locations.^{2,3} Also, a considerable amount of time is required to achieve steady-state vibration with low-frequency, lightly damped structures (e.g., 15 min for a 0.1 Hz mode with 0.5% damping). Phase separation methods based on frequency response functions are likewise generally unsuitable because of the time necessary to generate frequency spectra for such structures.⁴ Standard averaging procedures with random excitation can consume unacceptable amounts of energy, such as propellants for thrusters.

A feasible alternative to traditional test methods is time domain analysis of free-decay data.⁵⁻⁷ This approach is fast because only short transient responses are required (e.g., 30 s of data for a 0.1 Hz mode) and is simple because adequate excitation should be available from onboard devices such as thrusters or control-moment gyros. Several previous applications have demonstrated its potential. For these reasons, this approach was selected for future on-orbit experiments with Space Station Freedom.⁸

This paper consists of two parts. The first part discusses general issues concerning modal identification using free-decay data. This material is based on the experiences of the authors in several previous projects. The second part summarizes a recent laboratory application performed using impulse excitation and free-decay data. The test article is a simplified model of a generic space structure with flexible appendages. Modal parameters are identified using the eigensystem realization algorithm.^{9,10}

Environmental Constraints

Unique constraints are imposed by the harsh environment of space. Contrary to ground testing, ad hoc adjustments of sensors, exciters, or testing methodology will be costly or impossible to perform in space. The effects of the space environment must be carefully considered during test planning.

Temperature

Structures in space are exposed to extreme temperatures as well as large temperature gradients. Temperature gradients result from both the time-dependent transient from Earth shadow to sunlight (also called thermal shock) and local shaded areas adjacent to sunlight-exposed areas on the spacecraft due to its orientation to the Sun during traveling.

Unexpected temperature effects were observed in the Solar Array Flight Experiment (SAFE).^{5,11} The 31-m long structure was deployed from the cargo bay of Shuttle mission STS-41D

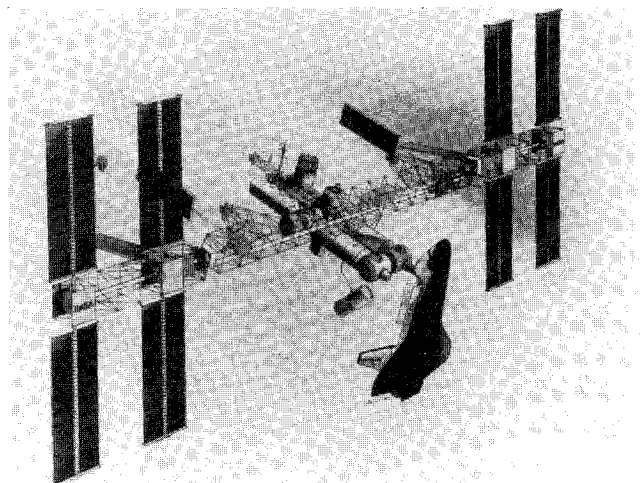


Fig. 1 Space Station Freedom.

Received April 26, 1991; revision received Dec. 2, 1991; accepted for publication Dec. 6, 1991. Copyright © 1991 by the American Institute of Aeronautics and Astronautics, Inc. No copyright is asserted in the United States until Title 17, U.S. Code. The U.S. Government has a royalty-free license to exercise all rights under the copyright claimed herein for Governmental purposes. All other rights are reserved by the copyright owner.

*Aerospace Engineer, Institute of Aeroelasticity, Bunsenstr. 10.

†Aerospace Engineer, Spacecraft Dynamics Branch, Mail Stop 297.

in September 1984. During dynamic testing the temperature alternated between -80 and $+75^{\circ}\text{C}$. At low temperatures, an unexpected curling of the blanket occurred (see Fig. 2). The curvature was 44 cm in depth. Upon entering sunlight, the blanket became flat in about 10 min. Consequently, there were two different structural configurations during each orbit with different vibration behavior due to prestress.

Temperature can also affect measurement equipment. In SAFE, for example, the curvature of the blanket affected a remote sensing system. Solar array motion during darkness was measured using laser-illuminated targets on the blanket. The target images were expected to fall on distinct regions of a stationary sensor located in the cargo bay. However, some images appeared at unexpected locations on the sensor due to the curvature of the blanket. This complicated the correlation of target images with corresponding positions on the blanket.

Accelerometer calibration is also affected by temperature. During daylight, some accelerometers will be much colder than others due to local shadowing. Continuous monitoring of sensor temperatures may be required to permit data corrections to be applied. Temperature variation effects can be minimized by acquiring data only during orbital night.

Background Disturbances

Modal identification using directly measured free-decay data assumes that no excitation occurs during the data acquisition period. With background disturbances, these assumptions are violated. Random disturbances cause modal amplitudes to fluctuate during the assumed free-decay period. Such fluctuations primarily affect damping estimates for weakly excited modes. Damping values can vary considerably and may even become negative.

Sinusoidal disturbances cause additional "modes" to be identified. Accuracy indicators for these results can be high because the signals are coherent over the measurement period. For complex structures with coupled motions, it can be difficult to differentiate these forced-response vibration patterns from true structural modes. Damping estimates, however, will be approximately zero due to the stationary character of the disturbance. Additional measurements should be made before and after each testing period to investigate the presence of disturbances and their significance.

Structural Characteristics

Complex large spacecraft possess nonuniform mass, stiffness, and damping properties. This results in coupled,

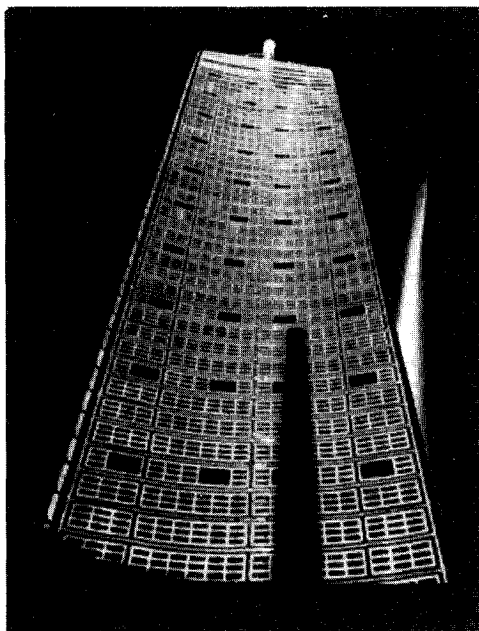


Fig. 2 SAFE, curled blanket.

three-dimensional vibration behavior with many closely spaced modes. Damping varies considerably in both magnitude and type due to diverse sources. Also, many types of nonlinearities can occur, including friction or backlash in joints and sloshing of propulsion fluids. Reliable methods for identifying primary modal characteristics in the presence of such complications must be developed.

Modal Density

Multiple excitation locations are necessary to identify closely spaced modes. Each excitation configuration corresponds to a different set of initial conditions. Response data can be analyzed in two different ways. In practice, each approach has advantages and disadvantages.

In the classical approach, each data set is analyzed separately. Various modes are determined better in various tests. Identification accuracy depends on the excitation selections and the resolution capability of the analysis algorithm. Linear combinations of modal parameters may be obtained when two or more closely spaced modes are excited and there is inadequate frequency separation. In the more modern approach, all available data sets are analyzed simultaneously using a multiple-input algorithm. Repeated eigenvalues of up to multiplicity m (i.e., m modes having identical frequency and damping values) can be identified if m independent sets of initial conditions are analyzed together.

Theoretically, the second approach is better for identifying closely spaced modes. In practice, however, data inconsistencies due to nonlinearities, slight changes in boundary conditions, stiffness variations due to temperature, etc., can cause difficulties for multiple-input analyses.¹⁰ Prudent practice is to use a combination of single-input and multiple-input analyses depending on the complexity of the structure and the consistency of data from various tests.

Damping

Modal identification becomes more difficult as damping levels increase. Higher damping decreases structural response magnitudes due to prescribed excitation forces. It also decreases signal-to-noise ratios over the free-decay measurement period. With localized damping sources, the damping distribution is nonproportional to the mass and/or stiffness distribution resulting in complex modes. It can be difficult in practice to differentiate true complex modes from modal complexity caused by identification approximations.¹²

With low damping, analysis directly in the time domain may be preferable to analysis of spectra or frequency response functions. In the latter approach, high frequency resolution is necessary for proper identification. High resolution requires long testing periods that conflict with the time constraints of on-orbit applications. A general disadvantage of low damping is that significant residual vibration may exist at the beginning of sequential testing periods. This causes response levels during the test to differ from those predicted using quiescent assumptions, raising possible safety concerns.

Nonlinearities

Various shaker locations excite modes to different amplitudes, causing shifting of modal parameters due to nonlinearities. Difficulties can occur during data analysis if these shifts are too large, particularly for closely spaced modes. With single-input analysis, nonlinearities complicate the correlation of results from separate tests. With multiple-input analysis, nonlinearities can cause numerical "mode splitting" due to inconsistent modal parameters for the various initial conditions. The magnitude and type of nonlinearity are generally different for different modes.

Structures can be "linearized" in ground tests using random excitation with averaging, sinusoidal excitation with bandpass filtering (to remove harmonics), or by mechanical means such as static preloads. The linear modal characteristics are then determined. In on-orbit tests, however, these methods are gener-

ally inapplicable. Reliable alternatives such as sliding time-window analyses must be developed and validated.¹⁰

Excitation and Sensing

Two requirements must be fulfilled to uniquely identify all modes: 1) controllability in the form of sufficient excitation and 2) observability in the form of an adequate number and distribution of sensors. In ground tests, complete controllability and observability can be achieved for all modes of interest. In space, however, fewer exciters and sensors will be available. Some modes will be weakly excited and/or observed. Data analysis techniques that assess the degree of controllability and observability must be used.

Controllability

Many considerations about possible sources of excitation for Space Station Freedom focused on the reaction control system (RCS).^{8,13} Certainly, one good reason to use RCS jet firings is the limitation of weight for additional exciters. The RCS is already aboard for attitude control and reboost to higher orbits. Unfortunately, these thrusters are located near the nodes of the fundamental truss bending modes to prevent large deflections of the spacecraft during firing. Furthermore, the strength of thrust is not adjustable and will vary over its lifetime due to a blowdown design. Separation of closely spaced modes that vary only in appendage in-phase and out-of-phase deformations but are similar in truss deformation may be impossible by means of such excitation.

The magnitude of modal response depends not only on the location and orientation of excitation sources but also on the time history of the applied forces. Single impulses, for instance, may produce inadequate response levels. If a sequence of pulses is applied instead, the input energy can be tailored to excite particular modes better. Care must be taken, however, not to select specific excitation frequencies only on the basis of predicted natural frequencies. Structural response with tuned excitation can be significantly less than expected for lightly damped structures due to errors in the predicted frequencies. On the other hand, if damping values are lower than anticipated, excitation near the natural frequency will produce higher response levels than expected.

Simulation results with Space Station Freedom showed that the success of on-orbit experiments is *most* sensitive to excitation locations and patterns.^{13,14} The locations and types of excitation forces are often varied in ground tests to achieve optimum results. This flexibility will generally be unavailable in on-orbit tests.

Observability

To achieve complete observability in ground tests, the number of sensors is typically 5 to 10 times the number of modes in the bandwidth of interest. As an example, 247 accelerometers were used to measure 43 modes of the ERS-1 satellite.³ The number of sensors in on-orbit tests of Space Station Freedom will be limited for practical reasons to less than 200. However, several hundred modes are predicted to occur below 10 Hz. The majority of these modes are associated primarily with appendage motion that is of secondary importance. Many of these "local" modes will have identical shape if sensed only on the primary structure.^{7,10} Additional measurements on the appendages are necessary to uniquely differentiate these motions.

Laboratory Application

The remainder of the paper discusses a recent laboratory application using time domain analysis of directly measured free-decay data. First, identification results obtained using all measured data are presented. This initial test is referred to as the "complete modal survey." As a simulation of an on-orbit experiment, the analyses are then repeated using a subset of

the available excitation and measurement locations. The findings are compared in the final section.

Test Structure and Data Acquisition

The test article for this investigation is shown in Fig. 3. In terms of modal characteristics it is dynamically similar to the truss/solar arrays of Space Station Freedom except that it has much higher natural frequencies. The structure consists of a cylindrical mast and four rectangular beams of various lengths. The beams are clamped at their centers to the tip and middle of the mast. One beam of each pair is additionally fitted with a constrained damping layer. The upper pair of beams is rotated 45 deg with respect to the lower pair. The overall dimensions are 1.59 m in height and 1.40 m in width, and the total mass is approximately 50 kg. This research structure was designed to provide specific dynamic characteristics including modal clusters, local response behavior, and damping coupling. These properties are representative of realistic spacecraft characteristics.

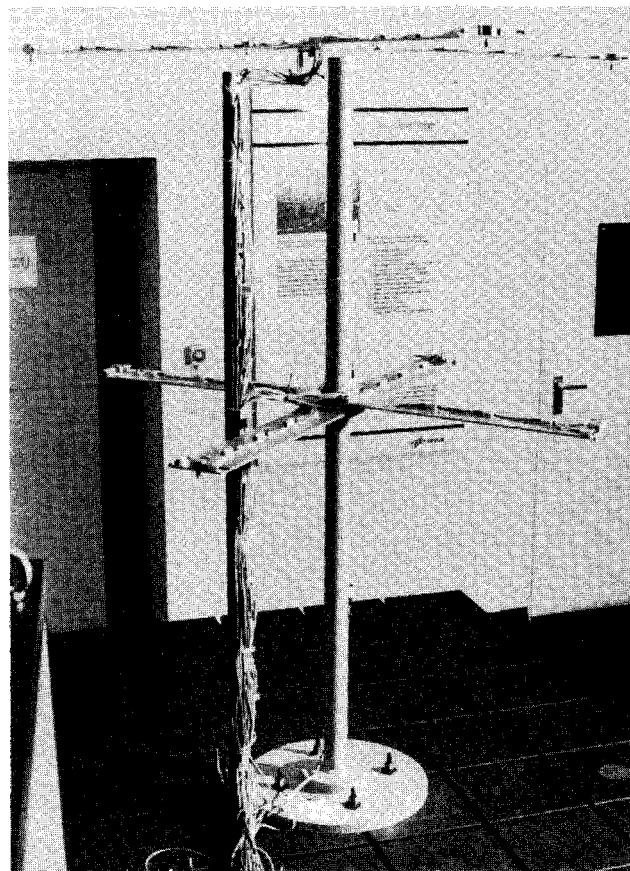


Fig. 3 Laboratory test structure.

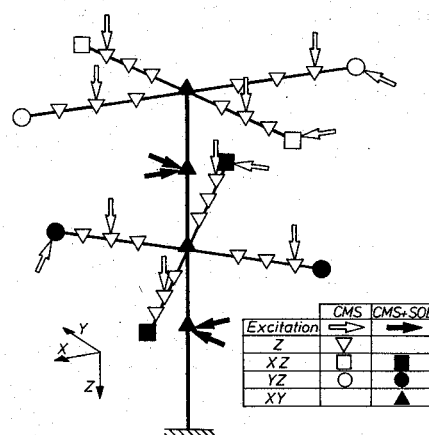


Fig. 4 Excitation and response locations.

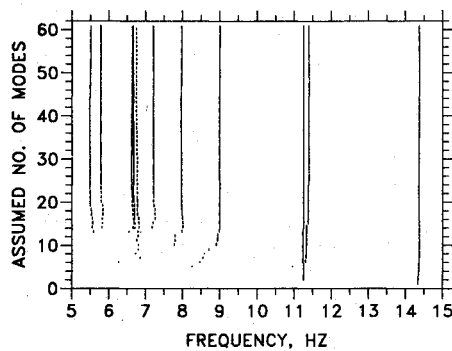
Excitation was performed manually using a rubber-tipped hammer. To excite all modes from 0 to 100 Hz, 16 separate single-point impacts were applied: 4 on the upper beams, 4 on the lower beams, 4 on the mast, and 4 in torsion. The response of the structure was measured with 48 accelerometers. The excitation and sensor locations are shown in Fig. 4. A force signal from the hammer triggered the data acquisition process. Each measurement period was 5.12 s long with a sampling frequency of 400 Hz. All data analyses were performed using only the free-decay portion of the measured responses.

With Space Station Freedom, direct force measurement will not be available for the thrusters. Only indirect approximation of force levels based on chamber pressures are possible. Therefore, the baseline on-orbit experiment uses free-decay response data only.^{8,13} These conditions are simulated in this laboratory application by not using force measurements in the modal identification analyses, although they are available.

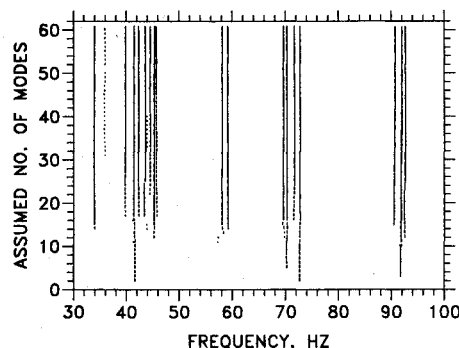
Complete Modal Survey

This section discusses modal identification results obtained by analyzing all measurements ($16 \times 48 = 768$ time histories) simultaneously. The results are considered "complete" in the sense that all available excitation and measurement locations are used. These findings provide a data base against which additional analyses of a simulated on-orbit experiment will be compared. Modal parameters are identified using the eigen-system realization algorithm (ERA).^{9,10}

Previous experience has shown that significant changes can occur in ERA analyses as a function of the assumed number of modes.¹⁰ Optimum accuracy for different modes typically occurs at different numbers of assumed modes. Also, weakly excited modes often require relatively high numbers of assumed modes to be properly identified. For these reasons, the assumed number of modes is incremented in each analysis from 1 to 60. The data are digitally filtered into two frequency bands to reduce numerical effort during analysis: 0–25 Hz and 20–100 Hz. Each filtered data set is analyzed separately. A data matrix size of 160 columns and 960 rows is selected. Default values for all other analysis parameters are used.⁹ These choices result in the use of 0.94 s of data in the 0–25 Hz range and 0.27 s of data in the 20–100 Hz range.



a) Lower frequency range



b) Upper frequency range

Fig. 5 Complete modal survey: identified frequencies.

The natural frequencies identified as a function of the assumed number of modes are plotted in Fig. 5. Each row corresponds to a separate analysis with a specified number of assumed modes. Each detected mode is represented by a vertical dash at the associated frequency. The confidence in each result is expressed by the length of the vertical dash that is proportional to the accuracy indicator known as the consistent-mode indicator (CMI).¹⁵ The highest confidence is attained if the distance between minor tick marks on the vertical axis is filled. Accordingly, for consistent identification over several separate ERA analyses, more confidence is associated with those results appearing as solid vertical lines than with those appearing as dotted or dashed lines. In practice, modes with CMI values greater than approximately 80% are identified with high confidence. A total of 30 modes are found in the frequency range from 0 to 100 Hz. With two exceptions at approximately 6.7 and 36 Hz, all modes are identified as straight and solid lines indicating consistency and reliability. Because of the trend of CMI to increase for most modes over the entire range of assumed modes, modal parameters for 60 assumed modes (the upper row in these plots) are listed in Table 1 together with CMI and the value of the phase resonance criterion (PRC).

PRC, also referred to as the "mode indicator function," provides an estimate of mode-shape accuracy.^{2,3} In theory, a value of 1000 indicates that the corresponding modal vector is entirely real; i.e., all response locations move exactly in-phase or out-of-phase with one another. This is a characteristic of classical normal modes. In practice, modes with values greater than 950 are considered to be well-identified normal modes. Twenty-three of 30 modes have values in this range. Three modes, nos. 3, 5, and 13, are identified with CMI less than 70% and PRC values lower than 900. Modes 3 and 5 predominantly involve bending of the upper damped beam. Because damping treatment is applied only to localized regions of the structure (two of the four beams), complex modes can occur and PRC values drop accordingly. Mode 13 is the most weakly excited of all identified modes. Low indicator values and un-

Table 1 Complete modal survey results

Mode no.	Frequency, Hz	Damping factor, %	CMI, %	PRC
1	5.513	1.614	88	986
2	5.780	0.211	93	985
3	6.643	1.306	66	786
4	6.665	0.156	95	991
5	6.752	1.233	41	768
6	7.211	0.316	93	985
7	7.979	1.448	89	968
8	9.005	1.767	95	994
9	11.252	0.095	99	991
10	11.390	0.103	98	991
11	14.369	0.049	98	995
12	33.974	1.487	82	975
13	35.916	2.906	30	871
14	39.885	0.225	88	986
15	41.493	0.195	95	984
16	42.354	0.136	91	989
17	43.604	0.208	89	958
18	44.542	1.198	81	960
19	45.428	1.348	87	983
20	45.707	0.150	73	909
21	58.141	0.349	88	994
22	59.197	0.322	85	982
23	69.605	0.500	92	939
24	70.260	0.364	93	951
25	71.685	0.083	85	976
26	72.749	0.078	92	984
27	90.725	0.848	85	975
28	91.993	0.694	70	911
29	92.028	0.143	76	941
30	92.647	0.246	81	969

usually high damping are attributed to identification scatter due to poor signal strength.

Another parameter used to estimate mode-shape accuracy is the modal assurance criterion (MAC).¹⁶ This parameter measures the similarity of mode shapes. Autocorrelation results for the modes listed in Table 1 are shown in Fig. 6 using a simple graphical format. Each row and column in the figure represents one mode shape. The MAC value is proportional to the size of the rectangle drawn at the intersection of the corresponding row and column. Values greater than 70% are darkened for emphasis. With few exceptions, all off-diagonal terms of the matrix are negligible, indicating uniqueness of the 30 identified modes.

In summary, a set of modal parameters believed to be complete in the 0–100 Hz frequency range is extracted from relatively simply acquired free-decay data. Accurate results are obtained for approximately 30 modes. These findings are corroborated by other tests performed with the classical phase resonance method using appropriated sinusoidal forces.¹⁷

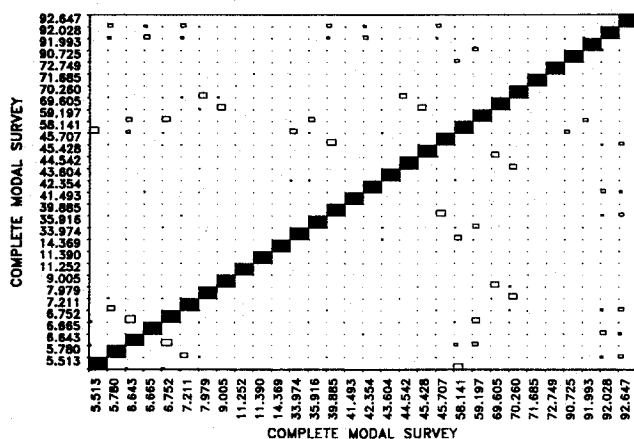
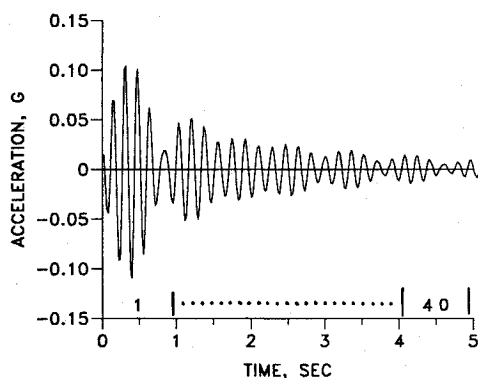
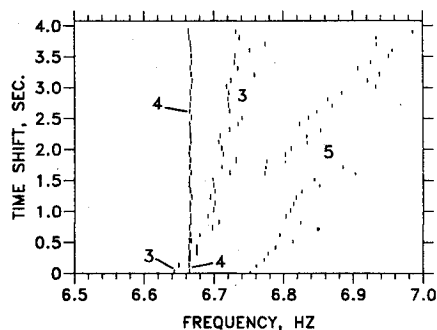


Fig. 6 Autocorrelation of identified mode shapes (using MAC).

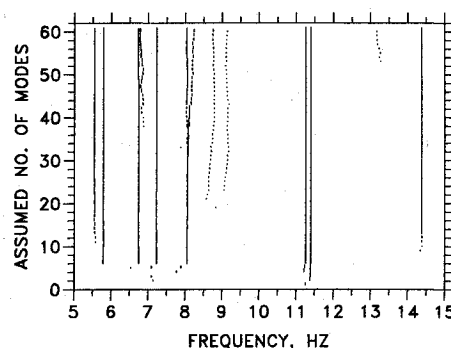


a) Procedure

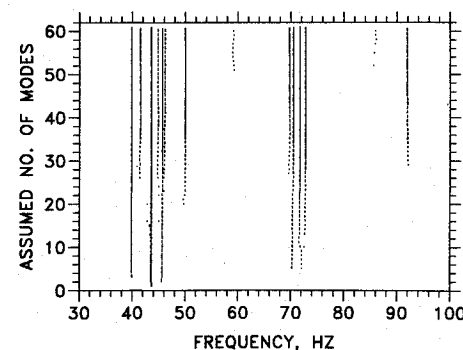


b) Identified frequencies near 7 Hz

Fig. 7 Sliding time-window analysis.



a) Lower frequency range



b) Upper frequency range

Fig. 8 Simulation of on-orbit experiment: identified frequencies.

Nonlinearity Study

Investigation of nonlinearities is possible with time domain methods using a sliding time-window analysis. Forty separate analyses are performed using a starting time varying from 0 to 4 s. The procedure is illustrated in Fig. 7a. Each analysis uses the same parameters as before, with 60 assumed modes.

Significant changes in identified natural frequencies occur as a function of response amplitude for modes associated with the damped beams. A typical result is shown in Fig. 7b. Mode 4 involves symmetric bending of the undamped upper beam. Its frequency is constant as a function of time shift (lower amplitudes occur at larger time shifts). The frequencies of modes 3 and 5, on the other hand, increase considerably. These modes involve symmetric bending of the damped upper beam. They are also highly coupled with mast bending. In mode 3 the two halves of the beam move in-phase with the mast whereas in mode 5 they move out-of-phase. As shown in Table 1, indicator values for modes 3 and 5 are unusually low. Nonlinearities combine with significant damping coupling to complicate reliable identification of these modes.

Simulation of an On-Orbit Experiment

Excitation for on-orbit experiments with Space Station Freedom will be provided by RCS thrusters attached to the truss.^{8,13,14} There are only two thruster locations. Response measurements will also be relatively sparse. Appendage measurements will be limited to tip and base locations only. Furthermore, some appendages may be uninstrumented.

These conditions of limited excitation and sensing were simulated by repeating the previous analyses retaining only 4 of the 16 excitation points and 16 of the 48 response points (see Fig. 4). Excitation was restricted to two locations on the mast in each of two directions, similar to the thruster locations of the space station. All eight response measurements on the mast were retained; however, on the appendages only eight measurements at the tips of the lower beams were kept. This selection of sensors matches one concept for the on-orbit experiment where the majority of sensors are located on the truss and only tip measurements are made on some solar arrays.

Based on the experience of the complete modal survey in terms of consistency and reliability of results, analyses are

repeated using the same variation of assumed modes from 1 to 60. The same size of data matrix is thus used. Because of the reduced number of excitations and responses, the time length data is accordingly increased to 2.4 s for filtered data from 0 to 25 Hz and 0.73 s for data from 20–100 Hz (vs 0.94 and 0.27 s, respectively, for the complete modal survey). If the same time length of data as in the complete modal survey is used instead, the data matrix size would be smaller in the present analysis. The desired variation of assumed modes up to 60 would then be impossible. With linear structures, longer data lengths increase modal identification accuracy (until the modal response level decays below the noise floor). With nonlinearities, however, identification accuracy can deteriorate with longer data records due to changing modal parameters as a function of response level. This is an example of a practical consideration necessary when different analyses are performed.

Identified natural frequencies for the on-orbit simulation are shown in Fig. 8. The same plot format as in Fig. 5 is used, and these two sets of results can be directly compared. Results obtained using 60 assumed modes are shown in Table 2 together with indicator values. Twenty-seven modes are now found. Besides many results with high consistency indicated by straight and solid lines, several others with shifting and dotted traces are present. Three modes at approximately 13, 59, and 86 Hz are detected only at high numbers of assumed modes. Based on PRC, 15 modes exhibit close to normal mode behavior with values higher than 950. On the other hand, nine modes have CMI less than 70%, and seven modes display considerable complexity with PRC values less than 900. "Mode splitting" occurs near 8 Hz at relatively high numbers of assumed modes. This indicates a lack of sufficient excitation and/or sensing or other sources of data inconsistencies. Considerable uncertainty is also associated with modes at 6.7 and 9 Hz. Modes in all three of these regions (6.7, 8, and 9 Hz) primarily involve motion of the damped beams. As discussed earlier, these modes are appreciably nonlinear.

In summary, with the reduced excitation and sensing in the simulated on-orbit experiment, there is a wide spread of accuracy and consistency in the results.

Comparison of Results

The performance of the simulated on-orbit experiment (SOE) is assessed in this section by comparing the results with those of the complete modal survey (CMS). Both frequency and mode shape correlation are necessary. The procedure is similar to that to be performed in on-orbit experiments except then the test results will be compared with analytical or dynamically scaled model predictions rather than with ground test results of the completely assembled full-scale structure.

The simulation results are not only a subset of those obtained in the complete test as may have been expected. Of course, several modes are missing (in the 30–50, 60, and 90 Hz

Table 2 Simulation of on-orbit experiment results

Mode no.	Frequency, Hz	Damping factor, %	CMI, %	PRC
1	5.550	1.453	84	951
2	5.791	0.357	96	960
3	6.731	1.942	76	981
4	6.782	1.836	74	968
5	7.221	0.331	93	937
6	8.033	1.789	81	986
7	8.229	1.256	56	941
8	8.751	1.286	47	821
9	9.134	2.319	14	710
10	11.258	0.080	99	991
11	11.394	0.090	98	996
12	13.169	1.070	19	791
13	14.380	0.077	93	976
14	39.892	0.076	99	989
15	41.497	0.447	68	948
16	43.592	0.220	96	987
17	44.814	1.373	56	977
18	45.677	0.141	75	882
19	46.202	0.872	54	915
20	49.976	0.005	81	889
21	59.140	1.147	21	765
22	69.722	0.575	78	961
23	70.484	0.346	90	988
24	71.710	0.118	96	979
25	72.738	0.094	93	998
26	85.975	1.109	13	848
27	91.937	0.700	71	931

ranges) due to the reduced number of excitation locations and sensors. In the complete test, there was a significant drop in CMI values from approximately 40% to less than 10%, clearly separating the 30 structural modes from additional "computational" modes. *In the SOE, however, no clear drop in CMI values occurred.* With some exceptions, indicator values have decreased. Surprisingly, several SOE modes are identified with higher accuracy indicators than their counterparts in CMS. This is explained by the local response behavior of the structure and the selection of optimal excitation and response locations for these modes by chance. Using all available responses in the complete survey, including those with poor signal-to-noise ratios, can result in lower indicator values for some modes. Improvements in identification accuracy can be achieved using optimal locations for excitation and sensing.

In addition to a comparison of Fig. 5 with Fig. 8 and Table 1 with Table 2, essential additional information is provided by the cross-correlation of mode shapes shown in Fig. 9. Compared with a unique correspondence of mode shapes as in Fig. 6, there are now several patterns of similarity in certain sections of the correlation plot. In a first section up to 9 Hz, multiple and high correlations exist among several modes, with MAC values up to 94%. The inadequate distribution of sensors prevents unique identification of modes with characteristic upper beam movements. However, these modes are indirectly identified due to the coupling of upper beam with mast deflection, which is similar for several modes. Such behavior of similar movement of a principal component in many modes is expected for any structure having multiple flexible appendages attached to a principal truss. Mode splitting is observed near 8 Hz in Fig. 8a. There are also two SOE modes at 8.75 and 9.13 Hz instead of only one mode at 9.0 Hz. Figure 9 clearly indicates that splitting has in fact occurred for SOE modes at 8.03 and 8.23 Hz. Surprisingly, the mode at 8.75 Hz is also similar in shape. All three of these modes correlate with that at 7.98 Hz, the most reliable of which is at 8.03 Hz based on indicator values. The mode at 9.13 Hz correlates uniquely with the CMS mode at 9.0 Hz.

This frequency range of multiple correlation is followed by unique correspondence of mode shapes between the two tests. Exceptions to this general behavior are the first and second torsional modes at 14.3 and 41.5 Hz, respectively. Both shapes

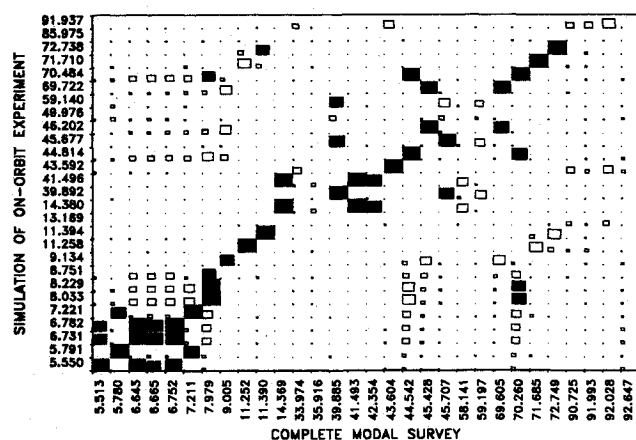


Fig. 9 Crosscorrelation of identified mode shapes (using MAC).

exhibit similar displacement patterns with the limited sensing in the simulation. Moreover, optimal excitation for these modes was not applied (only excitation at the mast was used in the SOE). However, both modes are clearly correlated with the corresponding complete results using both frequency and mode shape comparisons. Similar explanations are possible for modes at 44.8 and 70.5 Hz and at 46.2 and 69.7 Hz. These modes correlate with CMS modes at 44.5 and 70.3 Hz and at 45.4 and 69.6 Hz, respectively. A single mode above 90 Hz insufficiently correlates with three CMS modes in this frequency range. These three modes primarily involve motion of the upper beams that were uninstrumented in the simulation. The sensing of only the small residual movement of the mast caused this effect of ambiguous correlation.

Finally, there are three modes that do not correspond at all with CMS modes. Those at 13.2 and 86.0 Hz are weakly identified with CMI values of 19 and 13%, respectively. Recall that the data matrix size was kept constant in both tests. This results in longer data lengths in the simulation. Consequently, ambiguous modes can appear at large numbers of assumed modes, attributed to poor signal strength near the end of the data window. In contrast, the mode at 49.9 Hz is clearly identified with a CMI value of 81%. The associated low damping value discloses this mode to be electrical power noise.

In summary, 12 of 30 modes (40%) are uniquely identified in the simulation, taking into account mode shape correlation together with frequency comparisons. Another 13 modes (43%) can only be determined with multiple correlation. The five remaining modes are undetected in the simulation.

Conclusions

Traditional ground test methods will be difficult or even impossible to apply in space. Time domain analysis of directly measured free-decay data was discussed as a feasible alternative for on-orbit modal identification. Practical aspects concerning this approach were examined and illustrated in a recent laboratory application. A simulated space experiment was performed using a subset of available excitation and sensing locations. The success of this simulation can be summarized as follows: 40% of modes provided as a data base from a complete modal survey test are uniquely identified with less effort (25% in excitation and 33% in sensing); an additional 43% are identified only with nonunique correlation.

All findings indicate that on-orbit modal identification using directly measured free-decay data is possible. The success of such testing, however, is strongly dependent on sufficient excitation and an adequate distribution of sensing to cope with high modal density, various damping characteristics, local response behavior, and nonlinearities. Accuracy requirements for future space experiments are not yet fully available. This research contributes general information for preparation of the planned on-orbit experiments with Space Station Freedom.

Acknowledgment

This work was performed under a collaborative research agreement between NASA and DLR in the area of dynamics and control of large space systems.

References

- ¹Denman, E. D., Hasselman, T. K., Sun, C. T., Juang, J.-N., Junkins, J., Udawadia, F., Venkayya, V., and Kamat, M., "Identification of Large Space Structures on Orbit," American Society of Civil Engineers, AFRPL Rept. TR-86-054, New York, Sept. 1986.
- ²Niedbal, N., and Klusowski, E., "Optimal Exciter Placement and Force Vector Tuning Required for Experimental Modal Analysis," AIAA Paper 90-1205, April 1990.
- ³Degener, M., and Hüners, H., "Experiences with and Prospects for Dynamic Mechanical Testing of Spacecraft Structures," European Space Agency, ESA SP-304, June 1990, Paris, pp. 309-315.
- ⁴Allemang, R. J., and Brown, D. L., "Experimental Modal Analysis and Dynamic Component Synthesis," Air Force Wright Aeronautical Lab., AFWAL Rept. TR-87-3069, Eglin AFB, FL, 1987.
- ⁵Brumfield, M. L., Pappa, R. S., Miller, J. B., and Adams, R. R., "Orbital Dynamics of the OAST-1 Solar Array Using Video Measurements," AIAA Paper 85-0758, April 1985.
- ⁶Schenk, A., "Modal Analysis of Space Structures with the Ibrahim Time Domain Method," European Space Agency, ESA SP-289, Paris, Oct. 1988, pp. 293-299.
- ⁷Schenk, A., and Sinapius, M., "Identification of Operational Vibrations in Rail Vehicle Structures," *Proceedings of the 8th International Modal Analysis Conference*, Union College, Schenectady, NY, Jan. 1990, pp. 1262-1270.
- ⁸Cooper, P. A., and Johnson, J. W., "Space Station Freedom On-Orbit Modal Identification Experiment—An Update," *Proceedings of the 2nd USAF/NASA Workshop on System Identification and Health Monitoring of the Precision Space Structures*, Air Force Astronautical Lab., Edwards AFB, CA, March 1990, pp. 683-714.
- ⁹Juang, J.-N., and Pappa, R. S., "An Eigensystem Realization Algorithm for Modal Parameter Identification and Model Reduction," *Journal of Guidance, Control, and Dynamics*, Vol. 8, No. 5, 1985, pp. 620-627.
- ¹⁰Pappa, R. S., Schenk, A., and Noll, C., "ERA Modal Identification Experiences with Mini-Mast," *Proceedings of the 2nd USAF/NASA Workshop on System Identification and Health Monitoring of Precision Space Structures*, Air Force Astronautics Lab., Edwards AFB, CA, March 1990, pp. 331-370.
- ¹¹Young, L. E., and Pack, H. C., "Solar Array Flight Experiment/Dynamic Augmentation Experiment," NASA TP-2690, Feb. 1987.
- ¹²Özgüven, H. N., Imnegün, M., and Kuran, B., "Complex Modes Arising from Linear Identification of Non-Linear Systems," *Proceedings of the Florence Modal Analysis Conference*, Dept. of Mechanics and Industrial Technology, Florence, Italy, Sept. 1991, pp. 245-251.
- ¹³Kim, H. M., and Doiron, H. H., "Random Excitation Design for On-Orbit Modal Identification of Large Space Structures," Deutsche Gesellschaft für Luft- und Raumfahrt, DGLR Paper 91-081, Bonn, Germany, June 1991.
- ¹⁴Bleiloch, P., Engelhardt, C., and Hunt, D. L., "Simulation of On-Orbit Modal Tests of Large Space Structures," *Proceedings of the 8th International Modal Analysis Conference*, Union College, Schenectady, NY, Jan. 1990, pp. 926-932.
- ¹⁵Pappa, R. S., and Schenk, A., "A Consistent-Mode Indicator for ERA," AIAA Paper 92-2136, April 1992.
- ¹⁶Allemang, R. J., and Brown, D. L., "A Correlation Coefficient for Modal Vector Analysis," *Proceedings of the 1st International Modal Analysis Conference*, Union College, Schenectady, NY, Nov. 1982, pp. 110-116.
- ¹⁷Pappa, R. S., Schenk, A., Niedbal, N., and Klusowski, E., "Comparison of Two Dissimilar Modal Identification Techniques," Deutsche Gesellschaft für Luft- und Raumfahrt, DGLR Paper 91-078, Bonn, Germany, June 1991.

Earl A. Thornton
Associate Editor